# A molecular dynamics simulation study of the dimethyl sulfoxide liquid–vapor interface

Sanjib Senapati

**Articles you may be interested in**

Molecular dynamics simulation and identification of the truly interfacial molecules (ITIM) analysis of the liquid-vapor interface of dimethyl sulfoxide
J. Chem. Phys. **132**, 134701 (2010); 10.1063/1.3368111

Molecular-dynamics simulations of the ethanol liquid–vapor interface
J. Chem. Phys. **119**, 12569 (2003); 10.1063/1.1625643

Determination of curvature corrections to the surface tension of a liquid–vapor interface through molecular dynamics simulations
J. Chem. Phys. **116**, 302 (2002); 10.1063/1.1423617

Intermolecular interactions of liquid dichloromethane and equilibrium properties of liquid–vapor and liquid–liquid interfaces: A molecular dynamics study
J. Chem. Phys. **110**, 10113 (1999); 10.1063/1.478884

Structure, thermodynamics, and dynamics of the liquid/vapor interface of water/dimethylsulfoxide mixtures
J. Chem. Phys. **110**, 8070 (1999); 10.1063/1.478708

# A molecular dynamics simulation study of the dimethyl sulfoxide liquid–vapor interface

Sanjib Senapati
*Department of Chemistry, University of North Carolina at Chapel Hill, Chapel Hill, North Carolina 27599*

In this study, a fully flexible, nonpolarizable model potential of dimethyl sulfoxide (DMSO) has been used to investigate the DMSO liquid–vapor interface, based on classical molecular dynamics simulation techniques. A series of four simulations in the temperature range of 298–373 K is carried out to examine the temperature dependence of the structural, thermodynamic, and dynamical properties. The full Ewald summation technique is employed to account for the long-range electrostatic interactions. Computed bulk properties of the liquid such as density, diffusion are found to be in good agreement with experimental values. Self-diffusion coefficient of bulk DMSO molecules is computed to be smaller than at the interface. The study demonstrates the importance of inclusion of flexibility in the model and the use of Ewald sums, which have an influence on dynamics. © *2002 American Institute of Physics.* [DOI: 10.1063/1.1489898]

## I. INTRODUCTION

The equilibrium and nonequilibrium properties of the liquid interfaces have been the subject of considerable theoretical, computational, and experimental interest in the last several decades.[1–31] This is not surprising as these interfacial properties have direct relevance to various chemical phenomena like, the ion solvation at liquid interfaces, the isomerization reaction at liquid interfaces, interfacial charge transfer, and electron transfer reactions. These properties also play a critical role in understanding a variety of other processes including wetting, weathering, adhesion, lubrication, environmental science, and biological phenomena.

A large variety of modern experimental techniques including second harmonic generation,[1,2] sum frequency generation,[1,3] x-ray scattering,[4–6] neutron reflectivity,[7] and x-ray reflectivity[8] are used to obtain the structural and dynamical properties of these interfaces. However, because of the limited ability of these techniques to resolve many of the finer details of the interfaces, computer simulations and theories play a major role in developing our understanding in a more detailed manner and interpreting experimental observations. Mean-field theories[9,10] and integral equation theories[11–13] have been applied successfully to determine the liquid structure and thermodynamics at interfaces. Computer simulations also have proven to be useful tool for examining thermodynamic, structural, and dynamical properties of liquid–liquid,[14–19] liquid–vapor,[20–28] and liquid–solid interfaces[29–31] on a detailed microscopic level.

In this work, I am interested in the liquid–vapor interface of DMSO. DMSO is a polyfunctional molecule with a highly polar S═O group and two hydrophobic methyl groups. It is one of the most important aprotic dipolar organic solvents and also widely used cryoprotectant for biological structures like proteins and membranes.[32] It also has potential use in antiviral, antibacterial, and anti-inflammatory drugs.[33] These facts have spurred a wide variety of experiments on pure DMSO and DMSO–water

systems.[34–37] A few computer simulation studies are available on the bulk structure of DMSO[38–41] and water–DMSO mixtures.[42–44] However, the structure and dynamics of the DMSO liquid–vapor interface have not yet been examined.

DMSO is an important species in the atmospheric sulfur cycle.[33] Therefore, much of the interest of investigating the structure and dynamics of DMSO liquid–vapor interface is due to the role that this interface may play in atmospheric science. An understanding of the dynamics of molecules at the interface will be helpful in investigating the mechanism of adsorption of small solutes that are present in the atmosphere to the surface provided by this interface. Here I present the results of the molecular dynamics calculations of DMSO liquid–vapor interface. Results of particular interest include interface structure, the temperature dependence of surface tension, and the dependence of dynamics on both space and temperature.

The rest of the paper is organized as follows. In Sec. II, I describe the basic model used and the simulation details. The results of structural and thermodynamic properties are described in Sec. III. In Sec. IV, I describe the dynamical properties. Finally, the conclusions are summarized in Sec. V.

## II. THE MODEL AND SIMULATION DETAILS

A molecule of DMSO is represented by four interaction sites located on oxygen, sulfur and carbon atoms. The $CH_3$ groups are treated as unit sites. I have used the P2 model[42] of DMSO for the intermolecular interactions and a flexible model of DMSO proposed by Benjamin[43] for the intramolecular interactions. The flexibility is incorporated keeping in mind the fact that flexible models are more realistic and can introduce a significant effect on self-diffusion and other dynamical quantities. Benjamin who introduced the flexibility in the model of DMSO for the first time chose the intramolecular potential to reproduce the gas phase normal mode frequencies of the molecule. He then expected the P2 inter-

TABLE I. LJ parameters and partial charges for DMSO (Ref. 42).

| Atom | $\sigma$ (Å) | $\epsilon$ (kJ/mol) | $q$ (a.u.) |
|---|---|---|---|
| S | 3.4 | 1.00 | 0.139 |
| O | 2.8 | 0.30 | −0.459 |
| $CH_3$ | 3.8 | 1.23 | 0.160 |

TABLE III. Values of the parameters obtained in this work.

| $T$ (K) | $\rho_l$ (g/cc) | $z_L$ (Å)[a] | $z_R$ (Å)[a] | $t$ (Å) | $\gamma$ (mN/m) |
|---|---|---|---|---|---|
| 298 | 1.08 | −18.02 | 17.77 | 3.88 | 33.9±3.5 |
| 323 | 1.05 | −18.19 | 18.26 | 4.64 | 29.6±3.5 |
| 348 | 1.01 | −18.48 | 18.41 | 5.25 | 24.9±2.0 |
| 373 | 0.98 | −18.80 | 18.52 | 6.35 | 22.3±3.0 |

[a]$z_L$ and $z_R$ are the positions of the two Gibb's surfaces.

molecular potential model to shift the frequency to the proper condensed phase values. The interaction potential between $i$th and $j$th molecules is described as a sum of the Lennard-Jones (LJ) potential and Coulomb interactions of partial charges

$$U_{ij} = \sum_{\alpha} \sum_{\beta} 4\epsilon_{\alpha\beta}[(\sigma_{\alpha\beta}/r_{\alpha\beta})^{12} - (\sigma_{\alpha\beta}/r_{\alpha\beta})^6]$$
$$+ q_{\alpha}q_{\beta}/r_{\alpha\beta}, \qquad (1)$$

where $\alpha$ and $\beta$ stand for the sites in the $i$th and $j$th molecules, respectively. The cross interactions (i.e., LJ terms) are obtained by using the Lorentz–Berthelot combining rule. The LJ parameters along with the site charges ($q_{\alpha}$) are tabulated in Table I.

The intramolecular potential is represented by harmonic bond stretching and angle-bending terms. The related parameters are included in Table II.

For the present study, I perform a series of four molecular dynamics simulations on DMSO liquid–vapor system in the temperature range of 298–373 K. At each temperature, a cubic box with a linear dimension equal to 34.30 Å, and containing liquid DMSO is equilibrated for 200 ps in a NPT ensemble with a pressure of 1 atm (time constant 0.5 ps). This results in different box lengths for each of the temperature studied. After the equilibration, this slab of liquid phase is kept at the middle of the rectangular simulation cell with a slab of vapor at each end. Each slab of the vapor has $L_z = 35$ Å, and the same cross section as for the liquid slab. This geometry forms two interfaces perpendicular to the $z$ direction. The dimensions of the slabs are taken to be large enough to provide sufficient space for the bulk liquid and vapor densities to achieve constant values. This new system is then equilibrated in NVT ensemble for another 200 ps with initial velocities selected from a Maxwellian distribution. The systems are coupled to an external heat bath with a coupling time constant $\tau = 0.5$ ps. This last simulation provides the initial conditions for the production run of 500 ps in each system. Periodic boundary conditions are applied in three dimensions for all the simulations. The real space part of the Ewald sum and LJ interactions are cut off at 9 Å and

the simulation time step was 0.002 ps. Four simulations each consisting of 343 DMSO molecules are performed following this procedure at 298, 323, 348, and 373 K. The lengths of the simulation cells in the $x$ and $y$ directions are 34.28, 34.44, 34.72, and 35.05 Å for the simulations done at 298, 323, 348, and 373 K, respectively.

The production run consists of 10 blocks of 25 000 steps performed in the NVT ensemble. In each block, the density profile and self-diffusion coefficient are calculated every 100 steps. The data for the normal and tangential components of the pressure tensor are collected every 20 steps. The fluctuations are estimated using the variation in the block averages.

## III. STRUCTURAL AND THERMODYNAMIC PROPERTIES

I examine the number density profiles of DMSO molecules as a function of $z$ coordinates. The number densities are calculated by computing the average number of molecules in slabs of thickness $\Delta z = 0.2$ Å, lying on either side of the central plane at $z = 0$. Bulk values for the density are obtained from the plateau region of the density profiles and are tabulated in Table III. The bulk vapor density is calculated to be zero for all of the systems, therefore, not included in the table. A good agreement with the available literature values is found. For instance, the obtained liquid density of DMSO at 298 K is 1.08 g/cc, which is very close to the experimental value of 1.10 g/cc.[45] The very good agreement of the bulk values means that the systems are well equilibrated and the simulation procedures are correct. Figure 1 shows the number density profiles for the systems at 298 and 373 K. The profiles show two stable and smooth interfaces, thus indicating that the chosen potential model successfully describes the formation of liquid–vapor interfaces. Also, the liquid density at the bulk is found to decrease with increasing

TABLE II. Intramolecular interaction parameters for DMSO (Ref. 43).

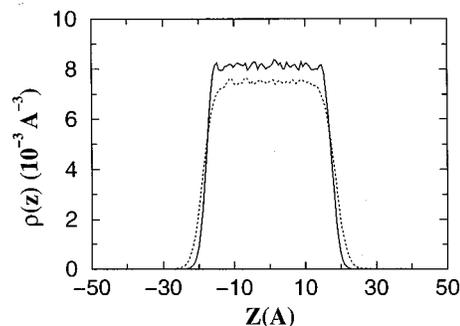| | |
|---|---|
| $k_{S-O}$ | 2510 kJ/mol Å$^{-2}$ |
| $r_{S-O}$ | 1.53 Å |
| $k_{S-C}$ | 1670 kJ/mol Å$^{-2}$ |
| $r_{S-C}$ | 1.80 Å |
| $k_{C-S-C}$ | 840 kJ/mol rad$^{-2}$ |
| $\theta_{C-S-C}$ | 97.4° |
| $k_{C-S-O}$ | 840 kJ/mol rad$^{-2}$ |
| $\theta_{C-S-O}$ | 106.75° |



FIG. 1. Average density profiles of DMSO at a temperature of 298 K (solid line) and 373 K (dotted line).

temperature as one expects. The interface on the other hand, becomes broader with increasing temperature.

One of the important properties characterizing the interface is the width. It arises due to the intermixing of two separate phases and is a strong function of temperature along with a few other state properties like surface tension and cross sectional area of the interface. Traditionally, the order parameter interfacial profiles have been fit with a hyperbolic tangent function to get a measure of the interface width. Therefore, I fit the calculated density profiles with a function of the following form,

$$\rho(z) = \frac{1}{2}(\rho_l + \rho_v) - \frac{1}{2}(\rho_l - \rho_v)\tanh\left[\frac{(z - z_o)}{d}\right], \quad (2)$$

where, $\rho_l$ and $\rho_v$ correspond to the liquid and vapor densities, $z_o$ is the position of the Gibb's dividing surface, and $d$ is a parameter for the thickness of the interface. The so-called "10–90" thickness, $t$, of a hyperbolic tangent function is related to $d$ by $t = 2.1972d$. The "10–90" thickness is the thickness over which the density of DMSO changes between 90% and 10% of the bulk value. The positions of the Gibb's surfaces and the values of the interface thickness obtained from the fitting are tabulated in Table III. The results show a strong dependence of the interface thickness on temperature.

From the thermodynamic point of view, a good quantity to characterize the interface is the surface tension. It is a measure of the degree of the structure possessed by the interface. When the interface is perpendicular to the $z$ axis, the surface tension ($\gamma$) can be defined as[19]

$$\gamma = \int_{-\infty}^{+\infty} dz[P_n - P_t(z)], \quad (3)$$

where $P_n$ and $P_t$ are normal and tangential pressures, respectively. For a planar interface, $P_n$ is uniform, however, $P_t$ depends strongly on position. At a point far from the interface, $P_t = P_n = P$. Therefore, only the region near the interface contributes to the integral. Let us define the averaged tangential pressure as

$$\bar{P}_t = \frac{1}{2L_z}\int_{-1/2L_z}^{+1/2L_z} dz[P_{xx}(z) + P_{yy}(z)], \quad (4)$$

where $P_{xx}(z)$ and $P_{yy}(z)$ are the components of the pressure tensor and $L_z$ is the length of the simulation box along $z$ direction. The surface tension in this case can be written as

$$\gamma = L_z(P_n - \bar{P}_t). \quad (5)$$

With two interfaces perpendicular to the $z$ axis, as in my systems, this equation transforms to

$$\gamma = \frac{1}{2}L_z(P_n - \bar{P}_t). \quad (6)$$

I have used Eq. (6) to obtain the surface tension values from the pressure calculations and the values are included in Table III. The dependence of it on temperature is shown in Fig. 2 along with the available experimental data.[45] A linear decrease in surface tension with increasing temperature is observed.
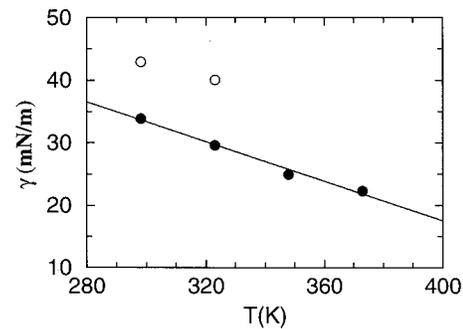


FIG. 2. The surface tension of dimethyl sulfoxide as a function of temperature. The solid circles represent the simulation results and the open circles represent the experimental data (Ref. 45).

However, the absolute values of surface tension underestimate the experimental values by about 20%. The result for surface excess entropy per unit area[46] defined as $d\gamma/dT$ also appears to underestimate the experimental data. For example, the calculated value for $d\gamma/dT$ is $-0.158$ mNm$^{-1}$ °C$^{-1}$, compared to the experimental value of $-0.114$ mNm$^{-1}$ °C$^{-1}$. It indicates that the present potential model which is more or less satisfactory for simulation of bulk liquid DMSO (e.g., it reproduces the experimental density and self-diffusion coefficient quite well) does not yield surface thermodynamic properties in very good agreement with experimental results.

## IV. DYNAMICAL PROPERTIES

In this section I report the dynamical properties of the DMSO molecules which have been investigated in the present work. The major objective has been to study the effects of temperature on translational self-diffusion coefficient. I am also interested to see the extent to which the dynamics of interfacial molecules differ from that in the bulk liquid phase at a given temperature. I have computed the velocity autocorrelation functions and from that have calculated the translational self-diffusion coefficients. The above dynamical quantities are calculated as a function of temperature and space. To compare the dynamical properties of the interfacial DMSO molecules with those at the bulk liquid phase, the entire system is divided into three regions. The region I (or the interfacial region) consists of molecules which are within the distance of 15–25 Å in the density distribution profiles (see Fig. 1), region II (or the diffuse interfacial region) includes molecules lying between 10 and 15 Å, and region III (or the bulk region) containing molecules that lie between 0 and 10 Å.

If I denote the velocity of a molecule at a time instance $t$ by $v(t)$ then the normalized autocorrelation function $C_v(t)$ can be defined as[47]

$$C_v(t) = \frac{\langle v(t)v(0)\rangle}{\langle v(0)^2\rangle}, \quad (7)$$

where $\langle\cdots\rangle$ represents an equilibrium ensemble average. The translational self-diffusion coefficient $D$ can be calculated from the velocity–velocity autocorrelation function by using the following relation:[47]
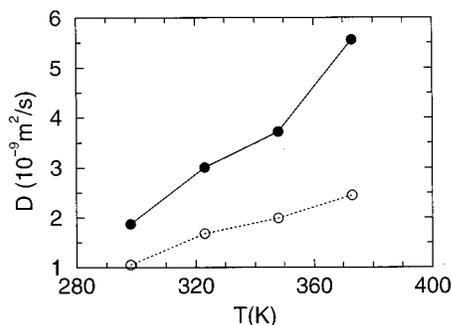
FIG. 3. The translational diffusion coefficients of DMSO molecules for the four systems studied in this work. The solid circles are for interfacial molecules and open circles for the molecules in the bulk region. The lines through the values are used to help the eye.

$$D = \frac{k_B T}{m} \int_0^\infty C_v(t)dt, \tag{8}$$

where $k_B$ is the Boltzmann constant, $T$ is the temperature, and $m$ is the mass.

I have calculated the self-diffusion coefficient of the interfacial and bulk regions using Eq. (8) for all the temperatures studied. The results are shown in Fig. 3. The presented diffusivity data for the interfacial regions correspond to the average value over all directions. The fluctuations associated with the average values vary from 5 to 10 percent of the reported values. The results of the diffuse interfacial region (region II) are not very different from the bulk phase results and, therefore, not included. The results imply that for all the systems the surface molecules diffuse in a faster rate than the molecules in the bulk phase. That is expected, since a molecule in the interfacial region feels a less effective friction due to the presence of fewer surrounding molecules compared to a molecule in the bulk phase which has dense surroundings. Diffusion coefficient values are also found to increase with increasing temperature for molecules in every region. This is due to the increased kinetic energy of the molecules. The same trend was seen for water liquid–vapor interfaces also.[23–26] A good agreement between the calculated and available experimental value is attained. For example, the calculated translational self-diffusion coefficient of liquid DMSO in bulk phase at 298 K is $1.05 \times 10^{-9}$ m²/s, compare to the experimental value of $0.8 \times 10^{-9}$ m²/s.[48] The self-diffusion coefficient for pure DMSO at 298 K using the P2 potential of DMSO has been evaluated by Skaff,[38] and by Liu et al.[39] Values of $1.2 \times 10^{-9}$ m²/s and $1.7 \times 10^{-9}$ m²/s were obtained by these authors, respectively. Albeit the present value still overestimates the experimental value, it gives better agreement compare to the values obtained by Liu et al. and Skaff. The difference between the present value and the value obtained by Liu et al. mainly stems from their neglect of those DMSO–DMSO interactions which occur beyond the 15 Å cut-off distance. Skaff, however, has calculated the DMSO–DMSO Coulombic interactions via the Ewald summation technique, as the present study does. The difference, however, arises from introducing flexibility in the model. Thus,

this paper enables a comparison of how the dynamics is affected by the use of Ewald sums and by introducing flexibility in the model.

## V. SUMMARY AND CONCLUSIONS

In this study, I have investigated the DMSO liquid–vapor interface by means of molecular dynamics computer simulations. A series of four simulations in the temperature range of 298–373 K has been carried out. Various structural, thermodynamics and dynamical properties are calculated and wherever possible compared with experimental data. The density profile shows the presence of distinct interfaces which become broader with increasing the temperature. Surface tension decreases linearly with increasing the temperature and the calculated values are found to underestimate the experimental values. The molecules in the interfacial region diffuse faster than the molecules in the bulk liquid phase, and the self-diffusion coefficient values increase monotonically with the temperature. The calculated self-diffusion coefficient value match well with the experimental result at 298 K.

The long-range dipole–dipole interactions between the DMSO molecules make an important contribution to the surface and dynamic properties. This paper enables a comparison of how the dynamics is affected by the use of Ewald sums to include the long-range interactions. It also demonstrates the importance of introducing flexibility in the model which has a significant effect on dynamics.

Good tests of the suitability of intermolecular potentials for the simulation study of surfaces, and effective modifications of available potentials to bring about better agreement with measured surface properties, would be helpful directions for further research. Work in these directions is in progress.

[1] K. B. Eisenthal, Annu. Rev. Phys. Chem. **43**, 627 (1992).
[2] M. C. Goh, J. M. Hicks, K. Kemnitz, G. R. Pinto, K. Bhattacharya, K. B. Eisenthal, and T. F. Heinz, J. Phys. Chem. **92**, 5074 (1988).
[3] Q. Du, R. Superfine, E. Freysz, and Y. R. Shen, Phys. Rev. Lett. **70**, 2313 (1993).
[4] C. Fradin, A. Braslau, D. Luzet, D. Smilgies, M. Alba, N. Boudet, K. Mecke, and J. Daillant, Nature (London) **403**, 871 (2000).
[5] M. Sanyal, S. Sinha, K. Huang, and B. Ocko, Phys. Rev. Lett. **66**, 628 (1991).
[6] I. Tidswell, T. Rabedeau, P. Pershan, and S. Kosowsky, Phys. Rev. Lett. **66**, 2108 (1991).
[7] J. Bowers, A. Zarbakhsh, J. R. P. Webster, L. Hutcandhings, and R. W. Richards, Langmuir **17**, 140 (2001).
[8] D. M. Mitriniovic, A. M. Tikhonov, M. Li, Z. Huang, and M. L. Schlossman, Phys. Rev. Lett. **85**, 582 (2000).
[9] A. Luzar, J. Chem. Phys. **91**, 3603 (1989).
[10] *Fundamentals of Inhomogeneous Fluids*, edited by D. Handerson (Marcel Dekker, New York, 1992).
[11] R. Evans, Adv. Phys. **28**, 143 (1979).
[12] S. Senapati and A. Chandra, Phys. Rev. E **59**, 3140 (1999).
[13] C. N. Patra and S. K. Ghosh, J. Chem. Phys. **106**, 2752 (1997).
[14] A. R. Van Buuren, S.-J. Marrink, and H. J. C. Berendsen, J. Phys. Chem. **97**, 9206 (1993).
[15] S. Senapati and M. L. Berkowitz, Phys. Rev. Lett. **87**, 176101 (2001).
[16] I. Benjamin, Annu. Rev. Phys. Chem. **48**, 407 (1997).
[17] T. Chang and L. X. Dang, J. Chem. Phys. **104**, 6772 (1996).
[18] Y. Zhang, S. E. Feller, B. R. Brooks, and R. W. Pastor, J. Chem. Phys. **103**, 10252 (1995).
[19] J. S. Rowlinson and B. Widom, *Molecular Theory of Capillarity* (Clarendon, Oxford, 1982).

[20] J. Alejandre, D. J. Tildesley, and G. A. Chapela, J. Chem. Phys. **102**, 4574 (1995).

[21] Y. L. Yeh, C. Zhang, H. Held, A. M. Mebel, X. Wei, S. H. Lin, and Y. R. Shen, J. Chem. Phys. **114**, 1837 (2001).

[22] J. G. Harris, J. Phys. Chem. **96**, 5077 (1992).

[23] R. S. Taylor, L. X. Dang, and B. C. Garrett, J. Phys. Chem. **100**, 11720 (1996).

[24] R. M. Townsend and S. A. Rice, J. Chem. Phys. **94**, 2207 (1991).

[25] S.-B. Zhu, T. G. Fillingim, and G. W. Robinson, J. Phys. Chem. **95**, 1002 (1991).

[26] M. Maroncelli and G. R. Fleming, J. Chem. Phys. **89**, 5044 (1988).

[27] S. W. Sides, G. S. Grest, and M. Lacasse, Phys. Rev. E **60**, 6708 (1999).

[28] M. A. Wilson, A. Pohorille, and L. R. Pratt, J. Phys. Chem. **91**, 4873 (1987).

[29] S. H. Lee and P. J. Rossky, J. Chem. Phys. **100**, 3334 (1994).

[30] X. Xia and M. L. Berkowitz, Phys. Rev. Lett. **74**, 3193 (1995).

[31] S. Senapati and A. Chandra, J. Phys. Chem. B **105**, 5106 (2001).

[32] T. J. Anchordoguy, C. A. Ceccini, J. N. Crowe, and L. M. Crowe, Cryobiology **28**, 467 (1991).

[33] S. W. Jacobs, E. E. Rosenbaum, and D. C. Wood, *Dimethyl Sulfoxide* (Marcel Dekker, New York, 1971).

[34] H. Bertagnolli, E. Schultz, and P. Chieux, Ber. Bunsenges. Phys. Chem. **93**, 88 (1989).

[35] A. Burneau, J. Mol. Liq. **46**, 99 (1990).

[36] U. Kaatze, M. Brai, F. D. Sholle, and R. Pottel, J. Mol. Liq. **44**, 197 (1990).

[37] B. C. Gordalla and M. D. Zeidler, Mol. Phys. **74**, 975 (1991).

[38] M. S. Skaf, J. Chem. Phys. **107**, 7996 (1997).

[39] H. Liu, F. Muller-Plathe, and W. F. van Gunsteren, J. Am. Chem. Soc. **117**, 4363 (1995).

[40] B. G. Rao and U. C. Singh, J. Am. Chem. Soc. **112**, 3802 (1990).

[41] A. Luzar, A. K. Soper, and D. Chandler, J. Chem. Phys. **99**, 6836 (1993).

[42] A. Luzar and D. Chandler, J. Chem. Phys. **98**, 8160 (1993).

[43] I. Benjamin, J. Chem. Phys. **110**, 8070 (1999).

[44] I. I. Vaisman and M. L. Berkowitz, J. Am. Chem. Soc. **114**, 7889 (1992).

[45] *CRC Handbook of Chemistry and Physics*, edited by D. R. Lide, 82nd ed. (CRC, Boca Raton, 2001–2002).

[46] C. A. Croxton, *Statistical Mechanics of the Liquid Surface* (Wiley, New York, 1980).

[47] M. P. Allen and D. J. Tildesley, *Computer Simulation of Liquids* (Clarendon, London, 1987).

[48] K. J. Packer and D. J. Tomlinson, Trans. Faraday Soc. **67**, 1302 (1971); E. Cebe, D. Kaltenmeier, and H. G. Hertz, Z. Phys. Chem., Neue Folge **140**, 181 (1984).